J|A|C|S
ARTICLES
Published on Web 01/31/2004

Electronic Structure of the Cysteine Thiyl Radical: A DFT and Correlated ab Initio Study

Maurice van Gastel,* Wolfgang Lubitz, Günter Lassmann, and Frank Neese*

Contribution from the Max-Planck-Institut für Bioanorganische Chemie, Stiftstrasse 34-36, D-45470, Mülheim an der Ruhr, Germany

Received October 1, 2003; E-mail: vgastel@mpi-muelheim.mpg.de; neese@mpi-muelheim.mpg.de

Abstract: The electronic structure and the unusual EPR parameters of sulfur-centered alkyl thiyl radical from cysteine are investigated by density functional theory (DFT) and correlated ab initio calculations. Three geometry-optimized, staggered conformations of the radical are found that lie within 630 cm^{-1} in energy. The EPR *g*-values are sensitive to the energy difference between the nearly-degenerate singly occupied orbital and one of the lone-pair orbitals (excitation energies of 1732, 1083, and 3429 cm^{-1} from Multireference Configuration Interaction calculations for the structures corresponding to the three minima), both of which are almost pure sulfur 3p orbitals. Because of the near degeneracy, the second order correction to the *g* tensor, which is widely used to analyze *g*-values of paramagnetic systems, is insufficient to obtain accurate *g*-values of the cysteine thiyl radical. Instead, an expression for the g tensor must be used in which third order corrections are taken into account. The near-degeneracy can be affected to roughly equal extents by changes in the structure of the radical and by hydrogen bonds to the sulfur. The magnitude of the hyperfine coupling constants for the β protons of the cysteine thiyl radical is found to depend on the structure of the radical. On the basis of a detailed comparison between experimental and calculated *g*-values and hyperfine coupling constants an attempt is made to identify the structure of thiyl radicals and the number of hydrogen bonds to the sulfur.

1. Introduction

Radical enzymes utilize amino acid radicals from protein side chains or cofactor radicals for their catalytic function. Such protein-associated radicals are tyrosyl, tryptophanyl, and cysteine thiyl radicals in case of oxygen-dependent radical enzymes and also glycyl radicals in case of anaerobic radical enzymes (for reviews see refs 1−4). Elaborate EPR studies have been performed on tyrosyl radicals in aerobic class I ribonucleotide reductase (RNR),[1,5] and in photosystem II,[1,3] on tryptophanyl radicals in cytochrome *c* peroxidase,[6] in DNA photolyase,[7] and in class I RNR,[8,9] as well as on glycyl radicals in anaerobic RNR,[10] and in pyruvate formate lyase.[11] In comparison to these radicals, however, the cysteine thiyl radicals have been explored to a much lesser extent.

Thiyl radicals play an important role in the catalytic mechanisms of all three classes of the radical enzyme RNR. In the aerobic class I RNR from *E. coli* (and mouse), a catalytically competent transient thiyl radical at Cys-439 of the R1 protein has been postulated to be formed from a stable tyrosyl radical at Y122 of the nonhaem iron containing R2 protein via a long-range proton-coupled electron transfer.[1,3,12,13] In anaerobic class III RNR, which carries an iron−sulfur cluster, a thiyl radical is discussed to be preceded by a stable glycyl radical.[4,10] Only in class II RNR from *Lactobacillus leichmannii*, a thiyl radical at Cys-208 which exhibits a strong magnetic interaction with a Co^{2+} complex, has been identified by EPR spectroscopy.[14] Furthermore, thiyl radical intermediates are postulated to play an essential role in biological sulfur insertion reactions for the generation of cofactors, e.g., in galactose oxidase and in biotin biosynthesis.[15]

Protein-associated cysteine thiyl radicals have been detected by EPR spin trapping techniques on hemoglobin following

(1) Stubbe, J.; van der Donk, W. A. *Chem. Rev.* **1998**, *98*, 705−762.
(2) Stubbe, J.; Nocera, D. G.; Yee, C. S.; Chang, C. Y. *Chem. Rev.* **2003**, *103*, 2167−2201.
(3) Sjöberg, B.-M. *Struct. Bonding* **1997**, *88*, 139−173.
(4) Fontecave, M. *Cell. Mol. Life Sci.* **1998**, *54*, 684−695.
(5) Gräslund, A.; Sahlin, M. *Annu. Rev. Biophys. Biomol. Struct.* **1996**, *25*, 259−286.
(6) Huyett, J. E.; Doan, P. E.; Gurbiel, R.; Housemann, A. L. P.; Sivaraja, M.; Goodin, D. B.; Hoffmann, B. M. *J. Am. Chem. Soc.* **1995**, *117*, 9033−9041.
(7) Gindt, Y. M.; Vollenbroek, E.; Westphal, K.; Sackett, H.; Sancar, A.; Babcock, G. T. *Biochemistry* **1999**, *38*, 3857−3866.
(8) Lendzian, F.; Sahlin, M.; MacMillan, F.; Bittl, R.; Fiege, R.; Pötsch, S.; Sjöberg, B.-M.; Gräslund, A.; Lubitz, W.; Lassmann, G. *J. Am. Chem. Soc.* **1996**, *118*, 8111−8120.
(9) Pötsch, S.; Lendzian, F.; Ingemarson, R.; Hörnberg, A.; Thelander, L.; Lubitz, W.; Lassmann, G.; Gräslund, A. *J. Biol. Chem.* **1999**, *274*, 17 696−17 704.
(10) Sun, X.; Harder, J.; Krook, M.; Jörnvall, H.; Sjöberg, B.-M.; Reichard, P. *Proc. Natl. Acad. Sci. U.S.A.* **1993**, *90*, 577−581.
(11) Knappe, J.; Elbert, S.; Frey, M.; Wagner, A. F. V. *Biochem. Soc. Trans.* **1993**, *21*, 731−734.
(12) Uhlin, U.; Eklund, H. *Nature* **1994**, *370*, 533−539.
(13) Mao, S. S.; Holler, T. P.; Yu, G. X.; Bollinger, J. M. jr.; Booker, S.; Johnston, M. I.; Stubbe, J. *Biochemistry* **1992**, *31*, 9733−9743.
(14) Gerfen, G. J.; Licht, S.; Willems, J. P.; Hoffman, B. M.; Stubbe, J. *J. Am. Chem. Soc.* **1996**, *118*, 8192−8197.
(15) Fontecave, M.; Ollagnier-de-Choutens, S.; Mulliez, E. *Chem. Rev.* **2003**, *103*, 2149−2166.

redox-reactions,[16,17] and on bovine serum albumine (BSA) and R1 protein of RNR upon thiol oxidation using a Ce^{4+} complex, or laser photolysis of nitrosylated thiols.[18] A direct EPR observation of protein thiyl radicals at low temperature was recently reported in UV irradiated frozen aqueous solution of BSA and R1 protein of RNR.[19,20]

EPR data are available for thiyl radicals of low-molecular weight thiols in disordered systems, e.g., solid powders or frozen solutions,[20−24] and single crystals after X- or UV irradiation at low temperatures.[25−32] The spectroscopic properties of thiyl radicals, such as the large and anisotropic *g*-factors, the strong and anisotropic relaxation, and the broad EPR lines, are unusual for a radical and reminiscent of a paramagnetic transition metal site. The large spin−orbit coupling of the sulfur atom was recognized as the general physical reason for these properties.[21] In a recent paper by Lassmann et al.,[20] a systematic study of the EPR spectroscopic properties of thiyl radicals in disordered systems, including protein-based thiyl radicals, was performed and phenomenological relationships between the *g*-values and the polarity of the solvent were established. Many open questions still exist, however, about the electronic structure of the alkyl thiyl radicals observed experimentally in cysteine moieties.

Although DFT calculations of the structure and/or magnetic resonance parameters were published for radicals from tyrosine,[33−36] tryptophan,[8] histidine,[37,38] and β-D-fructose,[39] only little information is available about the electronic structure of cysteine thiyl radicals. In a pilot MultiConfiguration Self-Consistent Field (MCSCF) and Density Functional Theory (DFT) study on EPR parameters of sulfur centered radicals by Engström et al.[40] on methanethiyl, the spread in *g*-values of the EPR signals were attributed to variations in the molecular environment, in particular the hydrogen bonds to the sulfur.

In this paper, we present an elaborate quantum-chemical study of the electronic structure of the thiyl radical and correlate the *g*-values and proton hyperfine couplings, which can be measured with EPR and related techniques,[20] to the structure and the environment of the radical. We found that the spectroscopic properties largely depend on the near-degeneracy of the singly occupied orbital of the unpaired electron and a sulfur lone-pair orbital, in-line with observations made earlier by Symons.[21] From a theoretical point of view, as a result of the near-degeneracy, we found that the *g*-values can only be understood if higher (third) order corrections to the expression of the *g* tensor are taken into account. The higher order effects are most pronounced for the g_z value (see Materials and Methods for the definition of the axes system), for which the second order correction, which is normally used, is negligible. Strikingly, we found that three stable conformations of the radical exist, two of which are close in energy ($\Delta E = 255$ cm^{-1}) and that the near-degeneracy of the orbitals can be affected to a large extent by the internal conformation of the cysteine. Hydrogen bonds to the sulfur can also influence the near-degeneracy, and the effect is comparable in size to that caused by changes in the conformation of the cysteine. By employing both the *g*-values and the proton hyperfine couplings from our calculations, we characterize experimental data for thiyl radicals in crystals of various cysteine derivatives and in disordered systems in terms of the structure of thiyl radicals and the number of hydrogen bonds to the sulfur.

2. Materials and Methods

For the cysteine thiyl radical we considered a molecular model that includes the complete amino acid, $S^{\bullet}CH_2CH(COOH)(NH_2)$. The axes system is chosen such that the *x* axis is parallel to the Cβ−Sγ bond direction and the *z* axis is in the Cα−Cβ−Sγ plane, where the positive direction is defined such that the *z* coordinate of Cα is more negative than that of Cβ and Sγ. In the calculations, in which the effect of the surrounding is investigated, the model also includes either one or two water molecules that form hydrogen bonds to the sulfur.

All DFT calculations are unrestricted calculations using the B3LYP functional. With the exception of the constrained geometry optimizations, they are performed with the ORCA program package.[41] For the complete geometry optimizations and frequency calculations the triple-ζ TZV basis set of Ahlrichs[42] is used, augmented with 2 sets of first polarization functions[43] on all atoms except hydrogen and with diffuse functions from the 6-311G++ basis set.[44,45] The convergence criteria for the SCF part are chosen to be 10^{-8} Hartree (Eh) for the change in energy, 10^{-7} Eh for the change of elements of the density matrix and 10^{-7} Eh for the maximum element of the Direct Inversion of Iterative Subspace (DIIS) error. A geometry is considered to be converged when

(16) Maples, K. R.; Kennedy, C. H.; Jordan, S. J.; Mason, R. P. *Arch. Biochem. Biophys.* **1990**, *277*, 402−409.
(17) Kelman,. D. J.; Mason, R. P. *Arch. Biochem. Biophys.* **1993**, *306*, 439−442.
(18) Kolberg, M.; Bleifuss, G.; Sjöberg; Gräslund, A.; Lubitz, W.; Lendzian, F.; Lassmann, G. *Arch. Biochem. Biophys.* **2002**, *397*, 57−68.
(19) Kolberg, M.; Bleifuss, G.; Gräslund, A.; Sjöberg, B. M.; Lubitz, W.; Lendzian, F.; Lassmann, G. *Arch. Biochem. Biophys.* **2002**, *403*, 141−144.
(20) Lassmann, G.; Kolberg, M.; Bleifuss, G.; Gräslund, A.; Sjöberg, B. M.; Lubitz, W. *Phys. Chem. Chem. Phys.* **2003**, *5*, 2442−2453.
(21) Symons, M. C. R. *J. Chem. Soc., Perkin II*, **1974**, 1618−1620.
(22) Sevilla, M. D.; Becker, D.; Yan, M. *Int. J. Radiat. Biol.* **1990**, *57*, 65−81.
(23) Gilbert, B. C. In Sulfur Centered Reactive Intermediates in Chemistry and Biology; Chatgilialoglu, C., Asmus, K. D., Eds.; Plenum Press: New York, 1990.
(24) Razskasowski, Y.; Becker, D.; Sevilla, M. D. In S-Centered Radicals; Alfani, Z. B., Ed.; John Wiley Sons: Chicester, 1999.
(25) Matsuki, K.; Hadley, J. H.; Nelson, W. H.; Yang, C.-Y *J. Magn. Reson. A* **1993**, *103*, 196−202.
(26) Akasaka, K. *J. Chem. Phys.* **1965**, *43*, 1182−1184.
(27) Box, H. C.; Freund, H. G.; Budzinski, E. E. *J. Chem. Phys.* **1966**, *45*, 809−811.
(28) Budzinski, E. E.; Box, H. C. *J. Phys. Chem.* **1971**, *75*, 2564−2570.
(29) Kou, W. W. H.; Box, H. C. *J. Chem. Phys.* **1976**, *64*, 3060−3062.
(30) Bonazola, L.; Fackir, L.; Levay, N.; Roncin, J. *Radiat. Res.* **1984**, *97*, 462−467.
(31) Saxebol, G.; Herskedal, O. *Radiat. Res.* **1975**, *62*, 395−406.
(32) Hadley, J. H.; Gordy, W. *Proc. Natl. Acad. Sci. U.S.A.* **1977**, *74*, 216−220.
(33) Blomberg, M. R. A.; Siegbahn, P. E. M. *Mol. Phys.* **2003**, *101*, 323−333.
(34) Himo, F.; Gräslund, A.; Eriksson, L. A. *Biophys. J.* **1997**, *72*, 1556−1567.
(35) Engström, M.; Himo, F.; Gräslund, A.; Vahtras. O.; Minaev, B.; Agren, H. *J. Chem. Phys.* **2000**, *104*, 5149−5153.
(36) Kaupp, M.; Gress, T.; Reviakine, R.; Malkina, O. L.; Malkin, V. G. *J. Phys. Chem. B.* **2003**, *107*, 331−337.
(37) Lassmann, G.; Eriksson, L. A.; Himo, F.; Lendzian, F.; Lubitz, W. *J. Phys. Chem. A* **1999**, *103*, 1283−1290.
(38) Lassmann, G.; Eriksson, L.; Lendzian, F.; Lubitz, W. *J. Phys. Chem. A* **2000**, *104*, 9144−9152.
(39) Pauwels, E.; Lahorte, P.; Vanhaelewyn, G.; Callens, F.; de Proft, F.; Geerlings, P.; Waroquier, M. *J. Phys. Chem. A.* **2002**, *106*, 12 340−12 348.
(40) Engström, M.; Vahtras, O.; Ågren, H. *Chem. Phys. Lett.* **2000**, *328*, 483−491.
(41) Neese, F. ORCA − An ab initio, Density Functional and Semiempirical program package, Version 2.2, revision 41, 2003, Max Planck Institut für Bioanorganische Chemie, Mülheim/Ruhr, 2003.
(42) (a) Schaefer, A.; Horn, H.; Ahlrichs, R. *J. Chem. Phys.* **1992**, *97*, 2571−2577. (b) Schaefer, A.; Huber, C.; Ahlrichs, R. *J. Chem. Phys.* **1994**, *100*, 5829−5835.
(43) TurboMole basis set library, available under ftp.chemie.uni-karlsruhe.de/pub/basen.
(44) Krishnan, R.; Binkley, J. S.; Seeger, R.; Pople, J. A. *J. Chem. Phys.* **1980**, *72*, 650−654.
(45) McLean, A. D.; Chandler, G. S. *J. Chem. Phys.* **1980**, *72*, 5639−5648.

the change in energy is less than 10^{-5} Eh, the average force is smaller than 5×10^{-4} Eh/Bohr and the maximum force is smaller than 10^{-3} Eh/Bohr. A frequency calculation has been performed following each geometry optimization in order to test whether the geometry corresponds to a local minimum on the potential energy surface. This is the case for all optimized structures (the smallest frequency was typically ~50 cm^{-1}). The zero point energies and thermal corrections have also been obtained from these calculations.

To calculate the excitation energy between the ground state and the first excited state, a spin-averaged Hartree−Fock (SAHF) calculation has been performed with three electrons in two orbitals, which is equivalent to a state averaged complete active space SCF (CASSCF) calculation in the same active space. Subsequently, a multireference configuration interaction (MR-CI) calculation within the recently developed Spectroscopy Oriented CI (SOR-CI) framework has been performed.[46] This method is a variation/perturbation approach and leads to a strong reduction in computational effort (the largest matrix to be diagonalized was only of dimension ~34 000), while it essentially maintains the accuracy of the MR-CI approach. MR-CI calculations of g-tensors were also considered by Lushington and a simplified procedure has been reported recently.[47] Our method, in addition removes the need for extensive basis sets since it is focused on accurate energy differences rather than accurate individual total energies. Although we used the relatively large IGLO-III basis set of Kutzelnigg et al.,[48] similar results were obtained with smaller basis sets. All calculations were executed within the ORCA package.

The *g* tensor and hyperfine tensor calculations are also performed with the IGLO-III basis set. The *g* tensor is calculated as a second derivative property by response theory. A description of the implementation is given in ref 49 and clear descriptions of the use of response theory are given in a.o. refs 50−56. In the hyperfine calculations, effective charges of 1, 3.6, 4.55, 5.6, and 13.6 are used for hydrogen, carbon, nitrogen, oxygen, and sulfur, respectively, to evaluate the spin−orbit contribution to the hyperfine tensor.[57] It is, in principle, not straightforward from an unrestricted Kohn−Sham calculation to interpret the orbital energies. We chose to present the orbitals as unrestricted natural orbitals, which are obtained from the diagonalization of the one-particle density matrix. A Löwdin spin-population analysis is performed on the natural orbitals and density plots are obtained by the program Molekel.[58] None of the calculations suffers severely from spin-contamination; the expectation value of the S^2 operator is typically 0.754.

B3LYP unrestricted constrained geometry optimizations with respect to the C−Cα−Cβ−Sγ dihedral angle have been carried out with Gaussian 98.[59] This angle has been varied from 0° to 360° in steps of 10° and all other coordinates have been optimized. The Ahlrichs triple-ζ basis set with polarization functions (TZVP) was used[42,43] in these calculations. SCF convergence criteria are 10^{-6} Eh and 10^{-8} Eh for the average and maximum change in the density. Geometry optimization convergence criteria are 4.5×10^{-4} Eh/Bohr and 3×10^{-6} Eh/Bohr for the maximum and average force, and 1.8×10^{-3} Bohr and 1.2×10^{-3} Bohr for the maximum and average displacements.

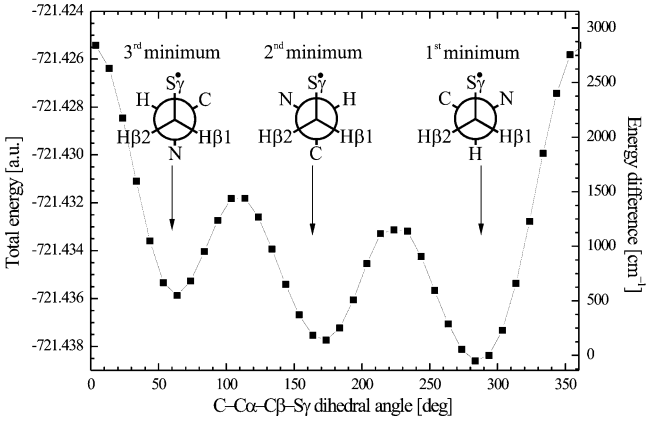

Figure 1. Potential energy surface for the cysteine thiyl radical resulting from a constrained geometry optimization with respect to the C−Cα−Cβ−Sγ dihedral angle.

3. Results

Upon inspecting the structure of the cysteine amino acid in the crystal structures of several proteins we noticed that there is a relatively large structural variation with respect to the rotation around the Cα−Cβ axis. This axis rotates the thiol group of the cysteine with respect to the backbone of the amino acid chain. Even within one protein the variations can be substantial. For example, inspection of the cysteines in the crystal structure of the [NiFe] hydrogenase of *D. gigas*,[60] yields values for this rotation (which we represent by the C−Cα−Cβ−Sγ dihedral angle) of 333° for Cys-65, 307° for Cys-68, 87° for Cys-530, and 164° for Cys-533. Part of the spread in these values probably stems from forces on the cysteine imposed by the protein, but the cysteine itself may also have a certain degree of flexibility with respect to the rotation around the Cα−Cβ axis. We investigated whether this is the case for the thiyl radical in vacuo by doing a constrained geometry optimization with respect to the C−Cα−Cβ−Sγ dihedral angle. The geometry of the cysteine thiyl radical was optimized with respect to all coordinates for fixed dihedral angles, which were scanned in steps of 10° from 0° to 360°. The energy surface with respect to this coordinate is given in Figure 1.

3.1 Geometry and Electronic Structure of the Cysteine Thiyl Radical. The curve shown in Figure 1 has three energy minima and three potential energy barriers between the minima. The minima correspond to conformations of the cysteine for which the atoms that are connected to the Cβ atom (the two β protons and the sulfur) are about 60° rotated with respect to

(46) Neese, F. *J. Chem. Phys.* **2003**, *119*, 9428−9443.
(47) Lushington, G. H. *J. Phys. Chem. A.* **2000**, *104*, 2969−2974.
(48) Kutzelnigg, W.; Fleischer, U.; Schindler, M. The IGLO-Method: Ab Initio Calculation and Interpretation of NMR Chemical Shifts and Magnetic Susceptibilities, Springer-Verlag: Heidelberg, **1990**, Vol. 23.
(49) Neese, F. *J. Chem. Phys.* **2001**, *115*, 11 080−11 096.
(50) Schreckenbach, G.; Ziegler, T. *J. Phys. Chem. A.* **1997**, *101*, 3388−3399.
(51) Pople, J. A.; Krishnan, R.; Schlegel, H. B.; Binkley, J. S. *Int. J. Quantum Chem.: Quantum Chem. Symp.* **1979**, *13*, 225−241.
(52) Malkina, O. L.; Vaara, J.; Schimmelpfenning, B.; Munzarova, M.; Malkin, V.; Kaupp, M. *J. Am. Chem. Soc.* **2000**, *122*, 9206−9218.
(53) Kaupp, M.; Reviakine, R.; Malkina, O. L.; Arbuznikov, A.; Schimmelpfenning, B.; Malkin, V. *J. Comput. Chem.* **2002**, *23*, 794−803.
(54) van Lenthe, E.; Wormer, P. E. S.; van der Avoird, A. *J. Chem. Phys.* **1997**, *107*, 2488−2498.
(55) Neyman, K. M.; Ganyushin, D. I.; Matveev, A. V.; Nasluzov, V. A. *J. Phys. Chem. A* **2002**, *106*, 5022−5030.
(56) Gauss, J.; Cremer, D. *Adv. Quantum Chem.* **1992**, *23*, 205−299.
(57) Koseki, S.; Schmidt, M. W.; Gordon, M. S. *J. Phys. Chem.* **1992**, *96*, 10 768−10 772.
(58) Molekel, Advanced Interactive 3D-Graphics for Molecular Sciences, available underhttp://www.cscs.ch/molekel/.
(59) Frisch, M. J.; Trucks, G. W.; Schlegel, H. B.; Scuseria, G. E.; Robb, M. A.; Cheeseman, J. R.; Zakrzewski, V. G.; Montgomery, J. A., Jr.; Stratmann, R. E.; Burant, J. C.; Dapprich, S.; Millam, J. M.; Daniels, A. D.; Kudin, K. N.; Strain, M. C.; Farkas, O.; Tomasi, J.; Barone, V.; Cossi, M.; Cammi, R.; Mennucci, B.; Pomelli, C.; Adamo, C.; Clifford, S.; Ochterski, J.; Petersson, G. A.; Ayala, P. Y.; Cui, Q.; Morokuma, K.; Malick, D. K.; Rabuck, A. D.; Raghavachari, K.; Foresman, J. B.; Cioslowski, J.; Ortiz, J. V.; Stefanov, B. B.; Liu, G.; Liashenko, A.; Piskorz, P.; Komaromi, I.; Gomperts, R.; Martin, R. L.; Fox, D. J.; Keith, T.; Al-Laham, M. A.; Peng, C. Y.; Nanayakkara, A.; Gonzalez, C.; Challacombe, M.; Gill, P. M. W.; Johnson, B. G.; Chen, W.; Wong, M. W.; Andres, J. L.; Head-Gordon, M.; Replogle, E. S.; Pople, J. A. Gaussian 98, revision x.x; Gaussian, Inc.: Pittsburgh, PA, 1998.
(60) Volbeda, A.; Garcin, E.; Piras, C.; de Lacey, A. L.; Fernandez, V. M.; Hatchikian, E. C.; Frey, M.; Fontecilla-Camps, J. C. *J. Am. Chem. Soc* **1996**, *118*, 12 989−12 996.

Scheme 1. Newman projections along the Cα−C*β* axis for the three structures that correspond to energy minima

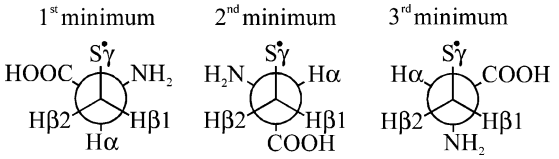

those connected to the Cα atom (the carboxyl carbon, the amide nitrogen and the α proton). This is illustrated by a Newman projection in Scheme 1.

The three minima on the potential energy surface correspond to such conformations and they are about 120° apart. In these minima, the cysteine is in a 'staggered' conformation, similar to the case of ethane, for which many extensive studies about the nature of the energy barrier are available.[61]

The three minima are close in energy. The energy difference between the 1st minimum and 2nd minimum is only 140 cm^{-1} (0.4 milliHartree (mEh)) and that between the 1st and 3rd minimum is 550 cm^{-1} (2 mEh). The energy maxima between the minima amount to 1150 cm^{-1}, 1450 cm^{-1} and 2700 cm^{-1}, respectively (which may be compared to the experimental and calculated values for ethane of 1023 cm^{-1} [62,63] and 912 cm^{-1},[61] respectively). In proteins, when the angle is different from either of these optimum conformations, the increase in the total energy of the cysteine may be compensated by favorable protein interactions. To find the optimum conformations of the thiyl radical in vacuo, we 'relaxed' the three geometries, i.e., we performed a full geometry optimization by using the three structures of minimum energy in the constrained optimization as starting points. The C−Cα−C*β*−S*γ* dihedral angles that correspond to the minima 1 to 3 are 286.6°, 171.3° and 61.4°, respectively, and the total energies of the 2nd are 3rd minimum are 255 cm^{-1} and 629 cm^{-1} higher than the total energy of the 1st minimum. The zero point energies and thermal corrections are within 30 cm^{-1} for the 1st and 2nd minimum. The zero point energy for the 3rd minimum is about 120 cm^{-1} larger than that for the 1st minimum, which increases the energy difference of the 3rd minimum and the 1st minimum, making the energy difference with respect to the structure of the 1st minimum 509 cm^{-1}. The optimized structure for the 1st minimum (286.6°) corresponds to that observed in the crystal structure of L(+) cysteine hydrochloride monohydrate.[64] The three structures are depicted in Figure 2. It is seen that the amide group and carboxyl group occupy different positions with respect to the $CH_2CS^{\bullet}$ moiety.

A selection of natural orbitals for the structure of the 1st minimum is shown in Figure 3a−f and their composition is given in Table 1. Orbitals a−d are doubly occupied (the occupation number is larger than 1.998). The singly occupied orbital (SOMO, e, with the occupation number exactly equal to 1.0[65]) is mainly localized on the sulfur and has dominant p_y character (85.9%). A small amount of density is present at the *β* carbon, and leads to a *π* antibonding interaction with the sulfur

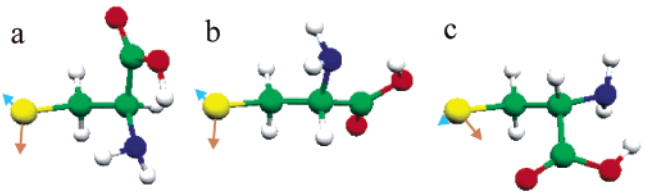

Figure 2. Overview of the three geometry-optimized structures of the cysteine thiyl radical, (a) 1st minimum, (b) 2nd minimum, and (c) 3rd minimum. The directions of the principal axes of the *g*-tensor: *z* (brown, parallel to the symmetry axis of the 3p orbital in the SOMO) and the y (light-blue) principal axis of the *g* tensor are indicated. The *x* axis is parallel to the C*β*−S*γ* direction.

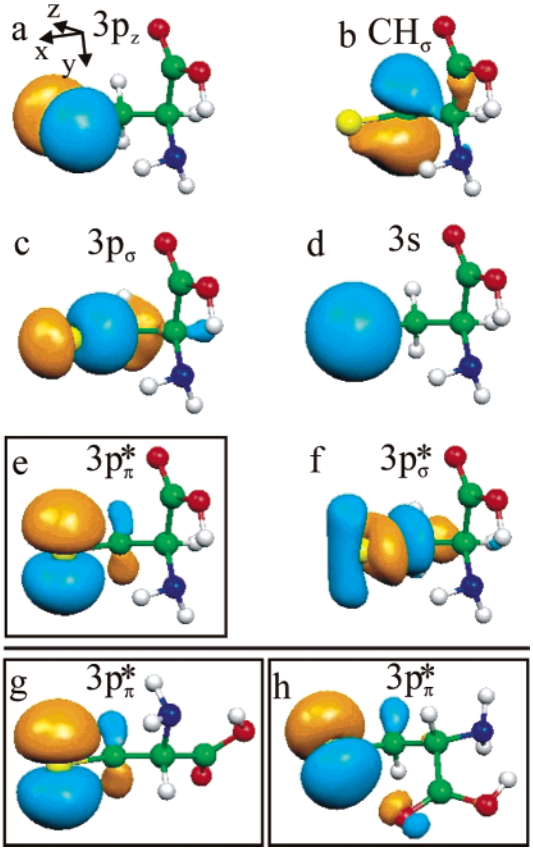

Figure 3. Overview of some natural orbitals for the conformation that corresponds to the 1st energy minimum; orbitals a−d are doubly occupied, e is singly occupied and f is empty. The *g*-values are largely dependent on the near-degeneracy of orbitals a and e. Orbitals g and h correspond to the singly occupied orbitals (SOMOs) of the conformations of the 2nd and 3rd minima. The diagrams for the singly occupied orbitals are highlighted by a black frame. The directions of the axes of the reference frame are indicated in panel a.

p_y orbital. The lone-pair orbitals of sulfur concern orbitals a and d. The orbital a is almost pure p_z (85.9%). Orbital d mainly consists of sulfur s character (75.1%) and a small amount of p_x character (10.9%) on the *β* carbon. Orbitals c and f describe the *σ*-bonding and *σ*-antibonding orbitals between sulfur and the *β* carbon. The natural orbitals compare well to those calculated by Guckert[66] with the SCF-Xα-SW method for SCH_3^-. Furthermore, from the composition of the natural orbitals, in which almost pure p and s orbitals on sulfur are present, it is clear that a simple picture in which the sulfur is sp^3 hybridized, does not give an accurate description, as is

(61) Goodman, L.; Gu, H.; Pophristic, V. *J. Chem. Phys.* **1999**, *110*, 4268−4275, and references therein.
(62) Pitzer, R. M. *Discuss. Faraday Soc.* **1951**, *10*, 66−73.
(63) Moazzen-Ahmadi, N.; McKellar, A. R. W.; Johns, J. W. C. *J. Chem. Phys.* **1992**, *97*, 3981−3988.
(64) Ayyar, R. R.; Srinivasan, R. *Curr. Sci.* **1965**, *15*, 449−450.
(65) Nakatsuji, H.; Kato, H.; Yonezawa, T. *J. Chem. Phys.* **1969**, *51*, 3175−3180.
(66) Guckert, J. A.; Lowery, M. D.; Solomon, E. I. *J. Am. Chem. Soc.* **1995**, *117*, 2817−2844.

Table 1. Composition [%] of Natural Orbitals (NO) for the Thiyl Radical in the Conformation of the 1*st* Energy Minimum (cf., Figure 2a). in the Last Column the Character of the Orbital Is Indicated

			Sγ				Cβ		Hβ(1)	Hβ(2)	
NO	occupancy	s	p_x	p_y	p_z	$d_{z^2-y^2}$	p_x	p_y	s	s	label
a	2				85.9						$3p_z$
b	2							47.5	22.8	9.1	CH_σ
c	2		44.3				38.5				$3p_\sigma$
d	2	75.1	7.3				10.9				3s
e	1			85.9							$3p_\pi$*
f	0		32.8			7.7	31.2				$3p_\sigma$*

Table 2. Summary of the C−Cα−Cβ−Sγ Dihedral Angles [deg], Excitation Energies $E_{0\rightarrow1}$ [cm^{-1}] from the Ground State to the First Excited State and *g*-Values for the Three Geometries that Correspond to Minima on the Potential Energy Surface[a]

	1st minimum			2nd minimum			3rd minimum		
∠C−Cα−Cβ−Sγ		286.6			171.3			61.4	
$E_{0\rightarrow1}$		1732			1083			3429	
	g_x	g_y	g_z	g_x	g_y	g_z	g_x	g_y	g_z
2nd order	2.2649	2.0215	2.0024	2.3692	2.0214	2.0023	2.1680	2.0161	2.0023
3rd order	2.2649	2.0043	1.9852	2.3692	1.9877	1.9686	2.1680	2.0092	1.9954
	x	*y*	*z*	*x*	*y*	*z*	*x*	*y*	*z*
$\angle(g_i,C\beta-S\gamma)$	1.3	88.7	89.9	1.6	89.5	88.5	2.6	89.7	87.4
$\angle(g_i,C\alpha-C\beta-S\gamma)$	347.7	170.3	80.3	53.8	174.7	95.3	121.2	37.6	127.6

[a] The *g*-values are calculated up to second order. Those up to third order result from eq 2. Also included are the angles [deg] between the principal axes ($i = x,y,z$) and the Cβ−Sγ direction, and the dihedral angle with the Cα−Cβ−Sγ plane. A graphical representation of the principal *y* and *z* axes is given in Figure 2.

already well-known for the heavier maingroup elements.[67] The s and d spin densities of sulfur amount to less than 1% and the p spin density is equal to 90%. The s spin densities at the β protons amount to 1.5% and 2.5%. In total, 3% spin density is present at the β carbon.

The SOMOs of the structures that correspond to the 2nd and 3rd minima are given in Figure 3g and 3h, respectively. The SOMO for the 2nd minimum is almost identical to that of the 1st minimum. The SOMO for the 3rd minimum has a different composition. The 3p orbital on sulfur has rotated and makes a sigma antibonding interaction with the oxygen from the nearby carboxyl group. The density on one of the β protons has become virtually zero. Excitation energies $E_{0\rightarrow1}$ from the ground state to the first excited state have been calculated for all three minima within the SOR−CI formalism. They are given in Table 2 and amount to 1732, 1083, and 3429 cm^{-1}, respectively. The excitation energies are a good measure for the degeneracy of the SOMO ($3p\pi$*, Figure 3e) and the doubly occupied orbital, which is closest in energy and called SOMO-1 ($3p_z$, Figure 3a). They show that the degeneracy is almost complete for the 2nd minimum and becomes less for the 1st and 3rd minimum, respectively.

3.2 The *g* Tensor, the Hyperfine Tensor, and the Effect of the Polarity of the Environment. For all three structures of the radical, *g* tensors have been calculated using response theory.[49] The *g* tensor is a property which can be measured by EPR spectroscopy and is usually dominated by spin−orbit coupling and the orbital angular momentum matrix elements between the SOMO and the other orbitals.[68] The calculated principal values and the directions of the principal axes of the *g* tensors for all three conformations are summarized in Table 2. It is seen that the *g* tensor is described by two *g*-values, g_z and g_y, close to the free electron *g* value ($g_e = 2.0023$) and one large *g* value, g_x. The large g_x value is determined by the matrix element $\xi_S\langle p_y|L_x|p_z\rangle\rangle \times \langle p_y\alpha|L_xS_x|p_z\alpha\rangle$ between the SOMO and SOMO-1 divided by the difference in energy of these two orbitals (ξ_S is the spin−orbit coupling constant of sulfur). Therefore, the principal axis that corresponds to the largest *g* value is almost parallel to the Cβ−Sγ direction (the *x* axis of the axes system, cf. materials and methods). Deviations of less than 2° were found for all three conformations. The principal *z* and *y* axes of the *g* tensor, included in Figure 2, are parallel and perpendicular to the symmetry axis of the p orbital on sulfur, which occurs in the SOMO. For the structure of the 3rd minimum, the *z* axis points toward the oxygen of the carboxyl group. The g_x values calculated with the B3LYP method amount to 2.2649, 2.3692, and 2.1680 for the three structures and the spread of these values is very large. The numbers correlate well with the MR-CI excitation energies (see Table 2, a small energy implies a large *g* shift), and show that the conformation of the backbone part of the cysteine is able to affect this degeneracy to such an extent that the shift of the g_x value with respect to g_e varies by more than a factor of 2!

Since the degeneracy of the sulfur p_z and p_y orbitals is of dominant importance for the shift of the g_x value, we investigated to which extent the near-degeneracy would be affected by the polarity of the surrounding solvent. For this purpose, we performed calculations for the thiyl radical in the presence of one or two water molecules that form a hydrogen bond to the sulfur. The geometries of these complexes have been optimized and hydrogen bond lengths (S...H) between 2.39 Å and 2.60 Å are found. Inspection of the orbitals revealed that the waters form hydrogen bonds to the $3p_z$ orbital (given in Figure 3a), by which this orbital is stabilized. The *g*-values have been calculated and are reported in Table 3. For the conformation that corresponds to the 1st minimum, the g_x value changes from 2.26 to 2.19 and to 2.14 for zero, one or two hydrogen bonds to the sulfur. For the conformations that correspond to the other two minima, similar trends are observed. The decrease in the g_x value indicates a lifting of the degeneracy of the p_z

(67) Kutzelnigg, W. *Angew. Chem., Int. Ed. Engl.* **1984**, *23*, 272−295.
(68) Atkins, P. W.; Jamieson, A. M. *Mol. Phys.* **1967**, *14*, 425−431.

Table 3. *g*-Values (up to second order) and Isotropic Hyperfine Coupling Constants (a_{iso}, MHz) for Both β Protons and ^{33}S for the Thiyl Radical Ligated by Zero, One or Two Water Molecules[a]

	1st minimum			2nd minimum			3rd minimum		
	0 H_2O	1 H_2O	2 H_2O	0 H_2O	1 H_2O	2 H_2O[b]	0 H_2O	1 H_2O	2 H_2O
g_x	2.2649	2.1974	2.1407	2.3692	2.2880	2.1952	2.1680	2.1205	2.0928
g_y	2.0215	2.0217	2.0212	2.0214	2.0217	2.0229	2.0161	2.0159	2.0156
g_z	2.0024	2.0024	2.0024	2.0023	2.0024	2.0025	2.0023	2.0024	2.0023
a_{iso}(H1)	90.8	92.3	91.1	85.5	96.1	112.2	11.2	5.0	6.6
a_{iso}(H2)	52.5	52.0	32.6	71.4	69.5	57.0	82.6	77.0	75.7
a_{iso}(^{33}S)	37.7	34.5	32.9	44.4	40.0	35.5	37.0	36.7	38.1

[a] The principal values of the anisotropic hyperfine tensor for both protons are typically (−4.5, −2.5, +7.0) MHz and vary by about 1 MHz depending on the number of water molecules surrounding the cysteine. The anisotropic hyperfine tensor for ^{33}S is (−85, −60, +145) MHz with a variation between the calculations of ±15 MHz. [b] Results in the table correspond to the geometry-optimized conformation as depicted in Figure 4a. For the conformation in Figure 4b the g-values amount to 2.4434, 2.0209 and 2.0025, the proton hyperfine values to 0.7 and 78 MHz and the ^{33}S hyperfine value to 52.8 MHz.

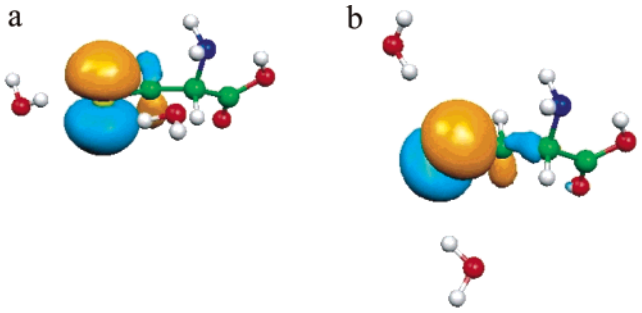

Figure 4. SOMO of the cysteine thiyl radical in the conformation of the 2nd minimum (analogous to Figure 3g), surrounded by two water molecules in different positions. The structure in a has been geometry optimized. The one in b is obtained by rotation of the two water molecules around the Cβ−Sγ axis.

and p_y orbitals, which is caused by both the hydrogen bond(s) of water to the cysteine and the electric dipole moment(s) of water. The decrease of the g_x value from 2.26 to 2.14 for the 1st minimum upon addition of two water molecules is comparable in size with the decrease of the g_x value when comparing the structure of the 1st and the 3rd energy minimum.

Obviously, both the conformation of the cysteine itself and the polarity of the solvent play an equally important role in determining the g_x value and small changes in either of them can change g_x considerably. To test this hypothesis, calculations have been performed for the cysteine thiyl radical with two water molecules whereby the waters have been artificially put at nongeometry-optimized positions. The *g*-values for the conformations of the 1st and 2nd minimum are very sensitive to changes in the positions of the water molecules and in one of the calculations the g_x value reached a value as large as 4.4, which indicates a breakdown of the perturbation procedure. In Figure 4, the SOMOs are given for the conformation of the 2nd minimum, for which the effect is most pronounced, with the waters in geometry optimized position (4a) and rotated about the Cβ−Sγ axis (4b). It is seen that the SOMO in Figure 4b has rotated with respect to that of Figure 4a and that the densities at the β protons, which were almost equal for the calculation with optimized geometry, have become very asymmetric (Table 3). The total energy of the structure in Figure 4b is 2200 cm^{-1} above that of Figure 4a, which is larger than the transition energy $E_{0\rightarrow1}$ (1083 cm^{-1}). Thus, for the conformations of the 1st and 2nd minimum, the two waters are able to completely lift the degeneracy and induce a large mixing between the SOMO and SOMO-1, whereas for the conformation of the 3rd minimum, the σ antibonding interaction with the oxygen of the carboxyl group (cf. Figure 3h) is of dominant importance. It is unlikely, however, that an energetically unfavorable structure like we used in the calculation presented in Figure 4b occurs in real systems.

Hyperfine coupling constants for the β protons and the sulfur (for the ^{33}S isotope, which has a nuclear spin 3/2) have also been calculated and the isotropic coupling constants are included in Table 3. For the β protons, the isotropic hyperfine coupling is dominated by the density of the SOMO at the position of the protons, which leads to large isotropic ^1H hyperfine couplings. Considerable anisotropy is introduced by the dipolar interaction with the spin density at the sulfur. For the conformation of the 1st minimum the isotropic ^1H hyperfine coupling constants are about 90 and 50 MHz, for that of the 2nd minimum 95 and 65 MHz and for that of the 3rd minimum 10 and 80 MHz. In the geometry-optimized calculations with water molecules, these numbers are affected to a limited extent (the largest difference exists for the 1st minimum with zero and with two water molecules, 52.5 and 32.6 MHz, respectively, cf. Table 3) and they are determined by the conformation of the cysteine itself. If the direction of the symmetry axis of the p orbital at sulfur in the SOMO is changed significantly by water molecules in a nonoptimum position, then the hyperfine coupling constants change. For example, the isotropic coupling a_{iso}(1) changes from 112 MHz to only 0.7 MHz when comparing the calculations for the thiyl radical in the conformation of the 2nd minimum with the water molecules in optimized (Figure 4a) and energetically unfavorable nonoptimized positions (Figure 4b).

The isotropic hyperfine interaction for ^{33}S is about 40 MHz with variations of 10 MHz depending on the number of water molecules present in the calculation and the particular geometry of the radical. The anisotropic ^{33}S hyperfine interaction is predicted to be much larger and has principal values of typically (−85, −60, +145) MHz, thus leading to principal values of the complete hyperfine tensor of (−45, −20, +185) MHz.

3.3 Third Order Correction to the *g* Tensor. The range of *g*-values found experimentally in various crystals and randomly oriented samples has been summarized in Table 4 and reproduced from ref 20. The g_x values span a range from 2.10 to 2.49 and most of them are close to either 2.25 or 2.15. This range of g_x values is reproduced well by our calculations. However, the calculations are not able to reproduce the experimentally found g_z value, which seems to be consistently smaller than the free electron *g* value (for some thiyl radicals, cf. Table 4, also the g_y value is smaller than 2.0023). In our calculations the *g*-values are calculated only up to second order in the spin−orbit coupling perturbation, which is usually sufficient for the interpretation of the experimental *g*-values.

Table 4. Experimental *g*-Values and Isotropic Hyperfine Parameters [MHz] for Both β Protons and ^{33}S for Thiyl Radicals in Single Crystals and Disordered Systems[a]

Compound, method	g-values			hyperfine coupling constants			ref.
	g_x	g_y	g_z	a_{iso}(H1)	a_{iso}(H2)	$a_{iso}(^{33}S)$	
Single crystals:							
Cysteine.HCl, e^-, 77 K	2.29	1.99	1.99	109	44		26
Cysteine.HCl, UV, 77 K	2.251	2.004	1.985	101	34		27
Penicillamine HCl, X, 4 K	2.297	2.037	1.921				28
	2.217	2.000	1.983				
Cysteine.HCl, X, 4 K	2.244	2.001	1.984	100.8			29
Cysteamine, γ, 77 K	2.242	1.999	1.980	92.4	42.0		30
1,4-Dithiane, γ, 77 K	2.224	2.028	1.999	95.2	33.6		30
N-acetylcysteine, e^-, 77 K	2.214	2.006	1.990	81.2	61.6		31
N-acetylcysteine, X, 77 K	2.214	2.006	1.990	81.2	61.6	43[d]	32
N-acetylcysteine, X, 4 K, H[g]	2.493	1.923	1.897	113		7[e]	25
N-acetylcysteine. X, 4 K, Y	2.164	2.012	2.003	110	55	[f]	
N-acetylcysteine, X, 4 K, Dd[c]	2.239	2.005	1.986	86	64	53[d]	
N-acetylcysteine, X, 4 K, K[c]	2.231	1.976	1.962	81	78	52[d]	
Frozen solutions/powder:	$g_{//}$	$g_\perp$					
BSA, 4 mM, pH 7, 20 mM ascorbate[b]	2.17	2.008					20
BSA, lyophilized	2.16	2.006					20
BSA, dry film	2.17	2.006					20
Cysteine. HCl, 300 mM, pH 3, 1 M LiCl, 10 min 140 K[b]	2.11	2.011					20
Cysteine. HCl, 300 mM, pH 3, 12 M LiCl, 10 min 150 K[b]	2.10	2.015					20
Cysteine, crystalline powder	2.15	2.011					20
Cysteine, 300 mM, pH 3[b]	2.30	2.008					20

[a] Also indicated is the method by which the radicals are created (X, γ, e^-, UV). [b] 200 mM phosphate buffer. [c] After annealing for 12 h at room temperature. [d] Recalculated after taking the appropriate signs of the principal values into account (see Table 3 for calculated values), i.e., the signs of principal values from the references have been changed to (199, −38, −32) MHz for the radical at 77 K, (200, −41, 0) MHz for Dd and (178, −23, 0) MHz for K. [e] Only observable at some orientations. Recalculated from principal values of (151, −78, −53) MHz. [f] No ^{33}S structure could be observed. [g] *N*-acetylcysteine radicals are named H, Y, Dd and K, following ref 25.

However, in the case of the near-degeneracy of the SOMO and SOMO-1, it is necessary to use a higher order expansion. General expressions for the third order correction to the *g* tensor are given by Atkins and Jamieson[68]

$$\vec{\vec{g}} = (2.0023)\vec{\vec{1}} - 2\xi \sum_m{}' \frac{\langle 0|\vec{L}|m\rangle\langle m|\vec{L}|0\rangle}{E_0 - E_m} + \frac{i\xi^2}{2} \sum_{mk}{}' \frac{\langle m|\vec{L}|k\rangle\cdot(\langle k|\vec{L}|0\rangle \times \langle 0|\vec{L}|m\rangle)\vec{\vec{1}} - 2\langle m|\vec{L}|k\rangle\langle k|\vec{L}|0\rangle \times \langle 0|\vec{L}|m\rangle}{(E_0 - E_k)(E_0 - E_m)} - \xi^2 \sum_m{}' \frac{\langle 0|\vec{L}|m\rangle\cdot\langle m|\vec{L}|0\rangle\vec{\vec{1}} - \langle 0|\vec{L}|m\rangle\langle m|\vec{L}|0\rangle}{(E_0 - E_m)^2} - \frac{i\xi^2}{\hbar^2} \sum_m{}' \frac{\langle 0|\vec{r}\,\vec{r}\,|m\rangle \times \langle m|\vec{L}|0\rangle}{E_0 - E_m} - \frac{1}{m^2c^2}\langle 0|p^2|0\rangle\vec{\vec{1}} \quad (1)$$

In this equation, the summation runs over all excited states, $\vec{L}$ is the orbital angular momentum operator, ξ is the spin−orbit-coupling constant, and $\vec{\vec{1}}$ is the 3 × 3 unit matrix. The wave functions in the bra and the ket concern the singly occupied orbitals in the ground state (0) and in the excited states (m or k) and the energies are state energies. Since this equation is not implemented in any existing DFT program (two-component treatments exist, however, in which the spin−orbit correction is treated to infinite order. See e.g., ref 69), we consider a two-state model of the SOMO and the SOMO-1 and approximate them as atomic p_y and p_z orbitals on sulfur, respectively (see Table 2). Expression 1 simplifies considerably and becomes (neglecting also the last term of eq 1)

$$\vec{\vec{g}} = 2.0023\begin{pmatrix}1&0&0\\0&1&0\\0&0&1\end{pmatrix} + 2k\alpha\begin{pmatrix}1&0&0\\0&0&0\\0&0&0\end{pmatrix} - k^2\alpha\begin{pmatrix}0&0&0\\0&1&0\\0&0&1\end{pmatrix} \quad (2)$$

where $\alpha \approx |\langle p_z|L_x|p_y\rangle|^2 = 1$ and k is the perturbation parameter, i.e., the spin−orbit-coupling constant of sulfur (382 cm^{-1})[70] divided by the energy difference of the ground state and first excited state. The second term is the dominant second order correction, which is positive and affects only the g_x value. The third term is the third order correction, which is negative and affects g_z and g_y. We have estimated the third order correction by calculating k from the second-order term (e.g., $k = 0.13$ for a g_x value of 2.26 for the 1st minimum without waters) and then inserting k into the expression for the third-order term. The resulting *g*-values are included in Table 2. Up to third order, the shift of g_z with respect to the free electron *g* value (and for the 2nd minimum also that of g_y) has indeed become negative and now falls within the range of the experimental g_z values. We therefore conclude that the negative shifts of the g_z values observed for cysteine thiyl radicals are the result of higher than second order contributions to the *g* tensor. For fully quantitative accuracy with respect to the experiment, one would have to go beyond third order.

3.3 Effect of (De)protonation of the Backbone. In the last paragraph, we discuss the effect of protonation of the amide group and/or deprotonation of the carboxyl group (zwitterionic

(69) (a) van Lenthe, E.; van der Avoird, A.; Hagen, W. R.; Reijerse, E. J. *J. Phys. Chem. A.* **2000**, *104*, 2070−2077. (b) Neyman, K. M.; Ganyushin, D. I.; Matveev, A. V.; Nasluzov, V. A. *J. Phys. Chem. A.* **2002**, *106*, 5022−5030.

(70) Carrington, A.; McLachlan, A. D. *Introduction to Magnetic Resonance*; Harper International: New York, 1967; pp 138−146.

structure). Calculations have been performed under these conditions and a significant shift of spin density (up to 30%) from sulfur to the amide/carboxyl group has been observed. Such a redistribution of spin-density is an artifact, however, which stems from the fact that the calculations are performed on radicals in vacuo. In reality, positive and/or negative charges on the protein backbone will be largely compensated by dipoles, charges and hydrogen bonds from the environment, that are absent in the calculation of the radical in vacuo. If, for example, in our calculation the amide group is protonated, the unpaired electron is 'attracted' to the additional amide proton and partly delocalizes to this group. On the other hand, if the carboxyl group is deprotonated, an excess of electron density is present at the oxygen. The electron density then shifts, in this case to the sulfur, leading to a decrease of the electron−electron repulsion. The net effect will be a redistribution of spin-density with an increase at the oxygen. Although it cannot be excluded that protonation of the amide group or deprotonation of the carboxyl group in thiyl radicals from isolated cysteine may have some effect on the g-values and hyperfine coupling constants presented in Tables 2 and 3, recent calculations for histidine radicals[37,38] and tryptophan radicals[8] showed good agreement between experiment and calculation with a nonzwitterionic model system in the calculations.

4. Discussion

With the information presented in the results section, i.e., (i) the fact that there are three structures for the thiyl radical, which correspond to local energy minima, (ii) the near degeneracy between the SOMO and SOMO-1, (iii) the sensitivity of the *g*-values to changes in these structures and the presence of hydrogen bonds to the sulfur, and (iv) the relative insensitivity of the hyperfine interaction of the β protons and the ^{33}S isotope to the hydrogen bonds, we are now in a position to compare our findings with the corresponding experimental quantities measured for thiyl radicals from cysteine or cysteine-containing proteins, either in frozen solution or embedded in single crystals. Before we start, it is worthwhile to mention that the g_x signals of thiyl radicals in disordered systems are usually broad and difficult to detect.[19,20] In a first quantum-chemical study of Engström et al.[40] on an $S^{\bullet}$-CH_3 model, the spread of the g_x values was attributed to variations in the molecular environment of the radical. Our results are in-line with these calculations and add to their results that a distribution of different conformations of the cysteine itself can have an equally large effect on the g_x values, and is therefore also an important factor that contributes to the experimentally observed line width.

4.1 Comparison of Calculated and Experimental *g* Values and Hyperfine Coupling Constants for Thiyl Radicals in Crystals and in Frozen Solution. The g_x values in Table 4 vary between 2.10 and 2.49. For thiyl radicals in single-crystals most g_x values are centered around 2.24 with a spread of 0.05, with the exception of *N*-acetyl-L-cysteine, for which four types of radicals were observed in a detailed experimental study.[25] The isotropic hyperfine interactions for the β protons in single crystals are typically 95 and 50 MHz with a spread of ±15 MHz. For randomly oriented thiyl radicals, most g_x values are concentrated around 2.15, the only exception being cysteine in frozen solution, for which the g_x value is reported as 2.30.[20] Unfortunately, no data for the hyperfine interaction of the β protons is available for thiyl radicals in disordered systems. Since the g_x value is sensitive to both the conformation of the cysteine and the environment of the sulfur, the g_x value alone is not a good indicator to characterize the conformation of the thiyl radical and the polarity of the environment around sulfur. Therefore, we focus our attention on the combination of the g_x value and the hyperfine interaction of the β protons, available for thiyl radicals in single crystals.

The size of the ^1H hyperfine coupling constants is dominated by the conformation of the cysteine thiyl radical itself. (Unless the waters are in such an energetically unfavorable position that the total energy is raised by more than the excitation energy of the ground state and the first excited state, cf. Results. It is clear from the small spread in the experimental hyperfine values, that this is not the case). The experimental isotropic hyperfine couplings agree well with the isotropic hyperfine couplings that have been calculated for the conformation that corresponds to the 1st energy minimum (cf. Table 3). This conformation is indeed present in crystal structure of L-cysteine in hydrochloride monohydrate. In the crystal structure a weak S−S interaction has been detected.[64] The latter observation does not one-to-one imply, that the radicals, after they are created by irradiation, also have this conformation. However, based on the combination of the g_x value of 2.25 and a_{iso}(H1,H2) ≈ 95,50 MHz, we attribute this data set to thiyl radicals in the conformation of the 1st energy minimum having a weak interaction with the environment (i.e., no hydrogen bonds).

For *N*-acetyl-L-cysteine crystals, a crystal structure is available.[71] The C−Cα−Cβ−Sγ dihedral angle is 291.9°, which indicates that the cysteines are in a conformation of the 1st minimum. However, four different thiyl radicals have been observed[25] in EPR experiments (see Table 4). After X-ray irradiation at low temperature, the so-called H and Y radicals are present.[25] For the thiyl radical Y, isotropic coupling constants of 110 and 55 MHz are reported with an anisotropic coupling $A_{//}$ of about 7 MHz. The isotropic coupling constants of the Y radical provide a strong indication that this radical has a conformation that corresponds to the one of our 1st energy minimum, and also the anisotropic coupling agrees with our calculation. The Y radical is characterized by a g_x value (2.16) and the negative shift of g_z and g_y are small. When comparing the experimental *g* value of 2.16 with the calculated ones for the 1st minimum in Table 3, the best agreement is found for a cysteine for which the sulfur has at least one hydrogen bond.

For the H radical, a broad doublet structure is present and only one set of hyperfine coupling constants has been extracted from the spectrum. The hyperfine splittings of the second proton leads to line-broadening.[25] The isotropic coupling is 113 MHz (cf. Table 4) and the anisotropic coupling constants are reported as (+7, ∼1, −7) MHz.[25] The H radical has a very large g_x value of 2.493 and the negative shifts of the g_z and g_y values are also very large. This correlates well with the expression for the *g* tensor in eq 2. If the second-order shift of the g_x value is large, then the third-order shift of the g_z and g_y values will also be large. A g_x value of 2.49 would result in g_z and g_y values of 1.94 within our simple model, which are close to the experimental values. The combination of a very large g_x value (2.493) and isotropic hyperfine coupling constants similar in magnitude is compatible with a conformation that corresponds to the 2nd

(71) Takusagawa, F.; Koetzle, T. F.; Kou, W. H. H.; Parthasarthy, R. *Acta Crystallogr. Sect. B* **1981**, *37*, 1591−1596.

energy minimum with no hydrogen bonds to the sulfur. The ^{33}S hyperfine interaction for the H radical is reported to be (53, 78, 151) MHz,[25] with the signals being only observable at some orientations. Given the spread of the calculated values with respect to a change in the geometry and the number of hydrogen bonds to the sulfur, the values come close to the ones of our calculation (−45, −20, +185) MHz, if one assumes the following sign of the principal values (−53, −78, +151) MHz. Note that the relative sign is difficult to determine from experiment and has been taken all-positive in ref 25. It is suspected that the experimental numbers have a rather large inaccuracy, which may explain the relatively large discrepancy. No ^{33}S hyperfine splitting was determined for the Y radical.[25]

After the *N*-acetyl-L-cysteine crystals are annealed at room temperature for 12 h and cooled again to 4 K, two new secondary thiyl radical signals appear (denoted Dd and K).[25] Both radicals have a g_x value of 2.23 and the hyperfine coupling constants for the β protons are also similar, 86 and 64 MHz and 81 and 78 MHz, respectively. The *N*-acetyl-L-cysteine thiyl radicals reported in another study at a temperature of 77 K[32] have essentially the same g and hyperfine values (see Table 4). The size of the proton hyperfine coupling constants indicates that these radicals have a conformation according to either the 1st or the 2nd energy minimum. Comparison of the g_x value with the ones for the 1st minimum in Table 3 indicates that both the Dd and the K radicals and the ones observed at 77 K would have a weakly hydrogen-bonded sulfur. Comparison of the g_x value with the ones for the 2nd minimum suggests that these radicals would need to have strong hydrogen bonds. Given the observation that the Y radical is in the conformation of the 2nd minimum and has no hydrogen bonds to the sulfur, the Dd and K radicals and the ones observed at 77 K are most probably in the conformation of the 1st minimum with a weak hydrogen bond to the sulfur. The signals related to the ^{33}S hyperfine interaction can be observed more reliably for the Dd and K radicals than those for the Y radical and much better agreement between experiment and calculation is found (cf., Tables 3 and 4).

We now turn our attention to thiyl radicals in frozen solution. Unfortunately, due to the large line width, no information about hyperfine couplings for either the β protons or the ^{33}S isotope is available. The decrease of the g_x value (∼2.15) as compared to that found in single-crystal studies (∼2.25), which is the result of partial lifting of the degeneracy of the p_z and p_y orbitals, indicates, that the thiyl radicals in solution have a more polar interaction with it's environment. According to Table 3, a g_x value of about 2.15 indicates that the radical is in the conformation of the 1st minimum and that the sulfur of the cysteine thiyl radical in frozen solution is hydrogen bonded. For cysteine in frozen solution ($g_x = 2.30$), it is in principle not possible to discriminate whether the conformation is as in the 1st minimum without hydrogen bonds to the sulfur or as in the 2nd minimum with at least one hydrogen bond to sulfur, although considering that all other cysteine thiyl radicals have a structure according to the one of the 1st minimum, the first possibility is most likely.

4.2 Third Order Correction to the *g* Tensor. Attempts have been made to analyze the *g*-values of the cysteine thiyl radical with a second-order expansion of the g tensor and the inclusion of 3d spin density at the sulfur.[32] Inclusion of sulfur 3d orbitals provides additional wave function coefficients that can be chosen such that the experimental *g*-values are reproduced, but at the price of having a large amount of 20% of 3d spin density at the sulfur.[32] We have not observed such 3d spin-densities in any of our calculations, and consequently, we believe that the *g*-values have to be explained by expanding the g tensor up to higher order in the spin−orbit coupling perturbation (cf. eq 1). The third order correction becomes important when the perturbation parameter, in this case equal to the spin−orbit-coupling parameter of sulfur divided by the energy difference between the SOMO (p_y) and the lone-pair (p_z) orbital, is not small. Because of the near degeneracy of these orbitals, this is the case for thiyl radicals and our model for the third order correction to the *g*-values yields good fits for the experimentally observed negative g_z and g_y shifts. The third order correction to the g_z and g_y values is most prominent, because the second order correction hardly affects this value (cf. Table 2 and eq 2), a situation which is reminiscent of that found in low-spin Fe^{III} complexes with a low-symmetry split $^2T_{2g}$ ground state.[72] In frozen solution, however, also the small g shifts are reported positive (i.e. the $g_\perp$ value is larger than g_e, see Table 4). For the systems with a perturbation parameter $k \approx 0.08$ ($g_x \approx 2.16$), this may be because of competition between a small positive second-order contribution (which is absent in our simple model, but present in the calculations, cf. Table 2) and the third-order contribution. Also it should be noted that the g_y and g_z values are difficult to resolve experimentally because of the line width and the possible presence of other radicals, and only $g_\perp$ is reported.

5. Summary and Outlook

The electronic structure of the cysteine thiyl radical has been calculated by density functional theory, using the B3LYP functional and a spin-unrestricted formalism. We found three local minima close in energy that differ with respect to a rotation about the Cα−Cβ axis. The singly occupied orbital is an almost pure $3p_y$ orbital on sulfur, which is nearly degenerate with the second lone-pair orbital, which is of almost pure sulfur-$3p_z$ type. The near-degeneracy causes exceptionally large g_x values in the EPR spectrum, which vary, depending on both the conformation of the cysteine itself and on the number of hydrogen bonds to the sulfur. This variation of the *g*-values (which was first discussed theoretically by Engström et al.[40]) explains the large experimental EPR line width in disordered systems, and also makes the *g*-values alone not well suited to identify the structure of the thiyl radical present in an actual system. From a theoretical point of view, the near-degeneracy of the sulfur p orbitals requires an expansion of the g tensor up to third order in the perturbation parameter. The third-order effect is most prominent for the g_y and g_z values, which have a negligible second order correction and for which values less than the free electron *g* value have been observed.

The hyperfine coupling constants for the β protons and the ^{33}S isotope are primarily determined by the structure of the cysteine thiyl radical itself. The combination of hyperfine values and *g*-values have been used to identify the structure of a number of cysteine thiyl radicals observed experimentally, and whether the sulfur is hydrogen bonded. Most thiyl radicals from cysteine

(72) Neese, F.; Zaleski, J. M.; Loeb-Zaleski, K. E.; Solomon, E. I. *J. Am. Chem. Soc.* **2000**, *122*, 11 703−11 724.

in frozen solution, including protein thiyl radicals, have a g_x value of about 2.15, which indicates a conformation according to the 1st minimum where the sulfur is hydrogen-bonded (an exception is cysteine 300 mM, pH 3 in 200 mM phosphate buffer with $g_x = 2.30$, which indicates the absence of hydrogen bonds). For thiyl radicals in crystals, the *g*-values are concentrated around 2.25 and a_{iso}(H1,H2) are about 95 and 50 MHz, which also indicates a conformation of the 1st minimum without hydrogen bonds. Here, the exceptions are the H and Y radicals of *N*-acetyl-L-cysteine. Y is hydrogen bonded based on the small g_x value of 2.16, H is in the conformation of the 2nd minimum without hydrogen bonds ($g_x = 2.493$). Although no cysteine−protein interactions have been taken into account in this work (which would vary depending on the protein under investigation and may have some influence on the *g* values), the present results may be used as reference data for the identification of the structure of thiyl radicals and may also contribute to the understanding of the catalytic cycle of radical enzymes in which thiyl radicals from cysteine side chains occur as intermediates.

Acknowledgment. This work was supported by the Max Planck Society, the DFG Priority Program on Molecular Magnetism (F.N.) and the Fonds der Chemischen Industrie (G.L. and W.L.).

Supporting Information Available: The coordinates of the cysteine thiyl radicals in the 1st, 2nd, and 3rd minimum. This material is available free of charge via the Internet at http://pubs.acs.org.

JA038813L